Atmos. Chem. Phys. Discuss., https://doi.org/10.5194/acp-2018-589
Manuscript under review for journal Atmos. Chem. Phys.
Discussion started: 24 August 2018

Atmospheric Chemistry and Physics Discussions

Comparison of Antarctic polar stratospheric cloud observations by ground-based and spaceborne lidars and relevance for Chemistry Climate Models

Marcel Snels[1], Andrea Scoccione[1], Luca Di Liberto[1], Francesco Colao[5], Michael Pitts[2], Lamont Poole[3], Terry Deshler[4], Francesco Cairo[1], Chiara Cagnazzo[1], and Federico Fierli[1]

[1]Istituto di Scienze dell'Atmosfera e del Clima, Via Fosso del Cavaliere 100, 00133 Roma
[2]NASA Langley Research Center, Hampton, Virginia 23681, USA
[3]Science Systems and Applications, Inc., Hampton, Virginia, 23666, USA
[4]University of Wyoming, Laramie, WY 82071, USA
[5]ENEA, Via Enrico Fermi 45, 00044 Frascati

Correspondence to: Marcel Snels (m.snels@isac.cnr.it)

Abstract. A statistical comparison of polar stratospheric clouds (PSCs) occurrence from 2006 to 2010 is presented, as observed from the ground-based station McMurdo (Antarctica), included as a primary station in the NDACC (Network for Detection of Atmospheric Climate Change), and by the satellite-borne CALIOP lidar measuring over McMurdo. The ground-based observations have been classified with an algorithm derived from the recent V2 detection and classification scheme, used to classify PSCs observed by CALIOP.

A statistical approach has been used to compare ground-based and satellite based observations, since point-to-point comparison is often troublesome due to the intrinsic differences in the observation geometries and the imperfect overlap of the observed areas.

This comparison of space-borne, ground-based lidar observations and a selection simulations obtained from Chemistry Climate Models. has been made by using a series of quantitative diagnostics based on the statistical occurrence of different PSC types. The distribution of PSCs over Antarctica, calculated by several CCMVal-2 and CCMI chemistry climate models has been compared with the PSC coverage observed by the satellite based CALIOP lidar. The use of several diagnostic tools, including the temperature dependence of the PSC occurrences, evidences the merits and flaws of the different models. The diagnostic methods have been defined to overcome (at least partially) the possible differences due to the resolution of the models and to identify differences due to microphysics (e.g. the dependence of PSC occurrence from T-T_{NAT}).

A significant temperature bias of most models has been observed as well as a limited ability to reproduce the longitudinal variations in PSC occurrences observed by CALIOP. In particular a strong temperature bias has been observed in CCMVal-2 models with a strong impact on PSC formation. The WACCM-CCMI model compares rather well with the CALIOP observations, although a temperature bias is still present.

Atmos. Chem. Phys. Discuss., https://doi.org/10.5194/acp-2018-589
Manuscript under review for journal Atmos. Chem. Phys.
Discussion started: 24 August 2018

Atmospheric Chemistry and Physics Discussions

1 Introduction

Lidar observations have been extensively used to characterize the occurrence of PSCs in the polar stratosphere (see e.g.Browell et al. (1990); Adriani et al. (2004); Di Liberto et al. (2014); Achtert and Tesche (2014)) . The observed optical parameters allow to discriminate different cloud types, such as STS (supercooled ternary solution), NAT (nitric acid trihydrate) and water ice, and external mixtures of the former. Pitts and co-workers (Pitts et al., 2009, 2011, 2013), calculated the optical parameters of cloud particles with different size distributions and chemical composition in order to define a PSC classification, which was then applied to the CALIOP data. Achtert and Tesche (Achtert and Tesche, 2014) made an assessment of several lidar-based PSC classifications and their impact on the occurrences of the different PSC types. Their conclusion was that the comparison of PSC classifications obtained from different lidar observations is not straightforward and should take into account the measurement technique and classification methodology used. Many different schemes have been proposed with thresholds for detection and classification, rendering a comparison difficult. Here we want to compare ground-based and satellite based lidar data, by using a detection and classification scheme for the ground-based data, which closely approaches the new V2 classification scheme used for CALIOP (Pitts et al., 2018).

Ground-based lidar observatories provide a unique data base, having decadal coverage, albeit with discontinuities, spanning from the early nineties to today. A clear issue is that the representativeness of ground-based long-term lidar data series of the Antarctic stratosphere might limit their value in climatological studies and model evaluation. The recent availability of satellite-borne lidar observations provides an almost complete coverage of the globe, and presents the opportunity to test the polar stratospheric cloud scheme of Chemistry Climate Models on synoptic scales. The Cloud-Aerosol Lidar and Infrared Pathfinder Satellite Observations (CALIPSO) was launched in April 2006 with the primary objective of improving our understanding about the impact of clouds and aerosol on the climate. The Cloud-Aerosol Lidar with Orthogonal Polarization (CALIOP) provides total backscatter and depolarization profiles, allowing classification of the observed clouds and aerosols. The original CALIPSO mission had a minimum time frame of 3 years, but has been extented several times and is still active.

Comparison between CALIOP and ground-based observations in the Antarctic stratosphere of PSCs is thus possible from 2006 on and has been pursued in the case of McMurdo Station by performing co-incident measurements with CALIPSO overpasses whenever possible.

Due to their primary role in ozone chemistry, a correct representation of PSCs in Chemistry Climate Models is needed. Actually, the parametrization of PSC formation in most CCMs depends only on temperature thresholds and on nitric acid and water vapour concentrations for the determination of supersaturation conditions. A rather complete description of the parametrizations used in state-of-the-art CCMs is reported in Morgenstern et al. (2017). The SPARC Report N^{o}5 (2010) Chemistry-Climate Model Validation (CCMVal-2) (Eyring et al., 2010) has shown that Chemistry Climate Models can have a biased representation of the stratospheric conditions with colder temperatures that lead to an overestimate of ozone depletion, also due to an unrealistic PSC coverage. Hence PSC simulations show a large uncertainty, as reported in the CCMVal-2 report. Nevertheless, the report presents a preliminary evaluation based on global averages with a subset of CALIOP data.

Atmos. Chem. Phys. Discuss., https://doi.org/10.5194/acp-2018-589
Manuscript under review for journal Atmos. Chem. Phys.
Discussion started: 24 August 2018

Atmospheric Chemistry and Physics Discussions

The most recent Chemistry Climate Models (CCM) are able to reproduce the denitrification by the formation of STS and NAT and the dehydration through the formation of ice clouds, but use rather approximate schemes based on temperature thresholds for the onset of nucleation, with additional constraints on how much of the available nitric acid is depleted by STS and NAT formation. Although the overall denitrification and dehydration can be represented rather well, the correct description of the formation of STS and NAT, and mixed type PSCs would need a more sophisticated microphysics model.

In the present work we first compare the statistics of occurrence of different PSC classes in the stratosphere over McMurdo station, as detected by the ground-based lidar operating there and the satellite-borne CALIOP. Subsequently we use the full coverage of the Antarctic CALIOP data to assess the performances of different CCMs in simulating PSC occurrences and PSC distribution over Antarctica.

2 Comparison of PSC observations by ground-based and satellite based lidars

2.1 CALIPSO PSC observations

The CALIPSO satellite was launched in April 2006 as a component of the A-train satellite constellation (Stephens et al., 2002, 2017). With an orbit inclination of 98.2 ^{o}, it provides extensive daily measurement coverage over the polar regions of both hemispheres, up to 82 ^{o} in latitude. It hosts the CALIOP (Cloud Aerosol Lidar with Orthogonal Polarization) two wavelength polarization diversity lidar, that measures backscatter at wavelengths of 1064 nm and 532 nm, the latter signal separated into parallel and cross polarization, with respect to the polarization of the outgoing laser beam. Details on CALIOP can be found in (Hunt et al., 2009; Winker et al., 2009). CALIOP data have extensively been used for observing PSCs and improved algorithms for PSC classification have been reported in Pitts et al. (2009, 2011, 2013).

2.2 Ground-based PSC observations at McMurdo

A Rayleigh polarization diversity lidar has operated in the Antarctic station of McMurdo since 1991, in the framework of an USA-Italian collaboration (Adriani et al., 2004; Di Liberto et al., 2014). It measures aerosol backscatter and depolarization profiles from 12 km to 30 km, with a vertical resolution of 30 meters. Aerosol backscattering is retrieved using the Klett algorithm and the extinction is calculated according to Gobbi (1995). The depolarization is calibrated following the method described in Snels et al. (2009). The lidar was operated by science technicians of the National Science Foundation (NSF) during the Antarctic winter, typically from the end of May until the end of September to cover the whole period of PSC occurrence. Potential vorticity reanalysis shows that McMurdo is well within the stratospheric polar vortex from mid-June to the end of September, except for rare events of major vortex perturbation. As a routine, the lidar is operated at the same time every day when meteorological conditions are favorable, or at the earliest chance to do so, for about 30 minutes to render a single profile. When possible, the observations are synchronized with overpasses of the CALIPSO satellite, when its footprint is within 100 km distance from McMurdo. Observations are intensified in coincidence with Optical Particle Counter (OPC) and ozonesondes balloon measurements (Adriani et al., 1992). All observations at a wavelength of 532 nm

Atmos. Chem. Phys. Discuss., https://doi.org/10.5194/acp-2018-589
Manuscript under review for journal Atmos. Chem. Phys.
Discussion started: 24 August 2018

Atmospheric Chemistry and Physics Discussions

used in the present analysis have been quality checked and the relevant data are publicly available in the NDACC data base (ftp://ftp.cpc.ncep.noaa.gov/ndacc/station/mcmurdo/ames/lidar/).

For the ground-based lidar data a single vertical profile with a vertical resolution of 150 m is obtained by averaging 30 minutes of acquistion. In order to facilitate the statistical analysis of the data, at most one profile is taken for each 6-hours time window.

2.3 PSC detection and classification

PSC detection and classification from lidar measurements with orthogonal polarization is usually based on two optical parameters derived from the optical signals with parallel and perpendicular polarization with respect to the laser, the backscatter ratio and the aerosol depolarization. The backscatter ratio is defined as

$$R = (\beta^{aer} + \beta^{mol})/\beta^{mol} \tag{1}$$

where β^{aer} is the total aerosol backscatter and β^{mol} is the total molecular backscatter.

If we define volume and molecular depolarization as

$$\delta^{vol} = \beta_{perp}/\beta_{par} \tag{2}$$

and

$$\delta^{mol} = \beta^{mol}_{perp}/\beta^{mol}_{par} \tag{3}$$

the aerosol depolarization can be expressed as (Cairo et al., 1999):

$$\delta^{aer} = \beta^{aer}_{perp}/\beta^{aer}_{par} = \frac{(1+\delta^{mol})\delta^{vol}R - (1+\delta^{vol})\delta^{mol}}{(1+\delta^{mol})R - (1+\delta^{vol})} \tag{4}$$

where β^{aer}_{par} and β^{aer}_{perp} are the parallel and perpendicular aerosol backscatter, respectively.

We must bear in mind that for all lidar measurements the optical parameters represent an average value of the microscopic properties of an ensemble of of many particles in a large air volume which may belong to different composition classes. Only rarely the observation of an air volume can be totally attributed to a single class of particles, except for particular cases where the temperature conditions exclude the co-existence of particles with different compositions. Thus the resulting macroscopic optical parameters are mostly due to external mixtures and are dominated by the species with the largest relative abundance and/or the largest optical parameters. When classifying the PSCs, the classifications indicate the dominant species or the mixtures of species.

Recently an overview of different detection and classification procedures has been reported by Achtert and Tesche (2014), showing how the different algorithms applied to the same data produce a variety of classifications. Here we limit the discussion to the data obtained by the CALIOP lidar and the McMurdo lidar observatory. Pitts and co-workers proposed a detection and

Atmos. Chem. Phys. Discuss., https://doi.org/10.5194/acp-2018-589
Manuscript under review for journal Atmos. Chem. Phys.
Discussion started: 24 August 2018

Atmospheric Chemistry and Physics Discussions

classification algorithm for PSCs in 2009 (Pitts et al., 2009), which has been slightly modified a few years later (Pitts et al., 2011). This algorithm used a classification of NAT mixtures in three classes, according to the different presence of NAT (Mix1, Mix2, Mix2-Enhanced). In 2013 an assessment has been performed on the PSC classification methods used (Pitts et al., 2013). In particular they examined the boundaries drawn between the composition classes and the causes of minor misclassifications and discussed the "cross-talk", meaning an overlap between composition classes in optical space, due to measurement noise. They observed that 5–6 % of PSCs classified as STS might actually be NAT mixtures, whereas only 1–2 % of PSCs classified as NAT mixtures might actually be STS. In this case the cross-talk was mainly due to the measurement noise for small values of β_{perp}. Their conclusion was that little cross-talk occurred between NAT-mixtures and STS, and that the ice assignment was very robust. On the other hand the separation of the NAT mixtures in Mix1, Mix2 and Mix2-enhanced classes was less reliable. This depends on the measurement uncertainties in R and δ^{aer} on one side and also on the location of the boundary between ice and NAT mixtures, which depends on the degree on denitrification (Pitts et al., 2013).

This classification method, with the exception of the mountain wave ice class has also been applied to a previous analysis of the McMurdo ground-based lidar data (Di Liberto et al., 2014).

2.4 PSC Detection and classification criteria for the CALIPSO V2.0 data

A new version V2.0 of the CALIPSO data based on a different algorithm has been made available recently (Pitts et al., 2018) and CALIOP data analyzed with this algorithm have been released as V2 CALIOP data. Here we compare these V2 data with ground-based observations at McMurdo from 2006 to 2010. The differences between V1.0 and V2.0 CALIOP PSC algorithms are listed below. Data pre-processing - Level 1 CALIOP data are now corrected for (minor) cross-talk between the parallel and perpendicular polarization channels. Uncertainties (“unc”) are calculated for all quantities based on the noise-scale factor (NSF) embedded in Level 1 data.

PSC detection - The thresholds for the background aerosol are now defined as the daily median plus one median deviation of 532-nm perpendicular backscatter (β_{perp}) and scattering ratio (R) of data at ambient temperatures above 200 K. PSCs are those data points for which β_{perp} or R exceeds the respective background threshold by more than unc(perp) or unc(R).

PSC composition - The former Mix1 and Mix2 classes have been combined into a single NAT mixtures class. The former Mix2-enhanced class has been renamed enhanced NAT mixtures and it now includes only those NAT mixtures with R > 2 and $\beta_{perp} > 2{\cdot}10^{-5}$ $m^{-1}sr^{-1}$. The wave ice class remains the same as in Version 1.0, i.e. ice PSCs with R>50. Each point detected as a PSC is assigned a non-spherical particle confidence index CI(NS) = [β_{perp} – unc(perp)] / unc(perp) and an STS confidence index CI(STS) = [R – unc(R)] / unc(R). If CI(NS) $\leq$ 1 and CI(STS) > 1, the PSC is classified as STS. If CI(NS) > 1, the PSC is presumed to contain non-spherical particles and is classified as a NAT (or enhanced NAT) mixture or ice based on its value of R. The position of the boundary separating ice from NAT (and enhanced NAT) mixtures, $R_{NAT|ice}$, is now calculated based on the total abundances of HNO_3 and H_2O vapors. These are determined on a daily basis as a function of altitude and equivalent latitude from nearly coincident cloud-free Aura MLS data. For estimating the total abundances of HNO_3 and H_2O, one should avoid MLS measurements that are impacted by uptake of vapour by PSC particles, since MLS only observes the gas-phase abundances. Since the MLS and CALIOP measurements are essentially co-located, all MLS profiles where CALIOP detects

Atmos. Chem. Phys. Discuss., https://doi.org/10.5194/acp-2018-589
Manuscript under review for journal Atmos. Chem. Phys.
Discussion started: 24 August 2018

Atmospheric Chemistry and Physics Discussions

the presence of clouds, have been ignored. So for each day, the mean HNO_3 and H_2O abundances have been calculated as a function of altitude and equivalent latitude only on MLS profiles in clear (cloud-free) air. Then each point containing non-spherical particles is assigned an NAT|ice confidence index CI(NAT|ice) = [R – $R_{NAT|ice}$]/ unc(R). For points classified as ice or wave ice, CI(NAT|ice) > 0. For NAT (or enhanced NAT) mixtures, CI(NAT|ice) $\leq$ 0.

The CALIOP V2 data set provide both the PSC classified grid according to the V2 algorithm and the associated optical parameters. From here on we will call the first CALIOP V2 PSC product and the latter CALIOP V2 data, for clarity.

2.5 PSC Detection and classification criteria for the ground-based data

In order to compare the ground based lidar data to the CALIOP data we have adopted a new algorithm which follows the same approach and uses the same optical parameters as the V2 CALIOP algorithm.

The ground-based raw data have been reelaborated to produce the backscatter ratio R and the perpendicular backscatter coefficient β_{perp}. The detection algorithm uses an average threshold of the backscatter ratio R_{thr} = 1.15, derived from the average signal to noise ratio of the lidar signals, and a threshold for β_{perp}, $\beta_{perp,thr}$ of $5{\cdot}10^{-7}$ $m^{-1}sr^{-1}$, estimated from observations without the presence of PSCs. All data with R > 1.15 or $\beta_{perp} > 5{\cdot}10^{-7}$ $m^{-1}sr^{-1}$, and a local temperature below 200 K in a range between 12 and 30 km are considered PSCs. Note that this procedure is essentially the same as the V2 algorithm for CALIOP data. Finally a coherence criterion has been applied, in order to avoid to detect isolated "spikes" as PSCs. This coherence criterion requires a continuity on the profile , i.e. in the vertical dimension, while the coherence criterion for CALIOP takes into account profiles along the flight track.

The PSCs are successively classified as STS, NAT mixtures, enhanced NAT mixtures and ice, by using similar criteria as reported for the CALIOP V2 algoritm. The discrimination between NAT mixtures and enhanced NAT mixtures is made by using the condition R > 2 and $\beta_{perp} > 2{\cdot}10^{-5}$ $m^{-1}sr^{-1}$, while the NAT|ice confidence index CI(NAT|ice) has been taken from the corresponding CALIOP data, since it is based on the total abundances of HNO_3 and H_2O vapors, and thus valid for CALIOP and ground-based data. We used monthly averages, since the variations during one month were not significant, and it largely simplified the procedure. The non-spherical particle confidence index CI(NS) = [β_{perp} – unc(perp)] / unc(perp) has been calculated from the standard deviation of the observed β_{perp} parameter. This procedure approaches the V2 algorithm applied to the CALIOP data as good as possible, and should provide a solid base for comparison.

2.6 Comparison of coincident PSC observations at McMurdo from the ground and from CALIPSO during the 5 year observation period

Here we compare PSC statistics from ground-based and satellite-borne lidars, with the goal to assess if their different measurement procedures induces a bias in the PSC classification, which might hamper the unique definitions of useful diagnostics for assessing the performance of regional and global models.

A comparison is made using 264 profiles acquired by the ground-based lidar and 8082 profiles extracted from the CALIOP data base within a 7^ox1^o longitude-latitude box centered on the McMurdo site for the years 2006-2010. The choice of the box dimension is dictated by the need to have a minimal latitudinal range (to avoid the inclusion of data in different vortex regimes

for stations close to the edge) and to have a significant number of observations (a larger longitudinal range assuming a local uniform distribution around the site).

The comparison between data obtained by space-borne and ground-based instruments is not straightforward. Lidars on satellites provide altitude resolved PSC observations on a synoptic scale, with fixed revisit times on the ground spot, and their observations in the stratosphere are unaffected by tropospheric visibility. Ground-based observations are limited by the weather conditions and become prohibitive in case of heavy cloud cover. Moreover the measurements occur once or twice per day, possibly in co-incidence with satellite overpasses. Sometimes they are conditioned by other activities such as intensive measurement campaigns of other instruments. The different geometry and measurement protocols might induce a bias in PSC statistics of ground-based and satellite-based lidar observations.

The ground-based lidar observes from distances up to 30 km from the ground, while the satellite based lidar is in orbit at 705 km and observes backscattering from distances around 700 km. This implies that the signal to noise ratio of CALIOP is in general lower than that of the ground-based lidar. Therefore the CALIOP data use averaging processes where the signal to noise ratio is low, and varies the threshold on both R and β_{perp} as a function of signal-to-noise ratio.

For these reasons, a point-to-point profile comparison of these data bases may not be sufficient to evaluate whether or not the instruments provide a compatible information of PSCs coverage and partition in different classes, which, at the end is the information needed to evaluate models and provide a climatic survey of the polar stratosphere.

In order to illustrate how ground-based and space-borne lidar observations of PSCs compare, we show as an example the height-time evolution of PSC classes for CALIPSO and McMurdo data bases for the year 2006 (see Figure 1), having the best temporal coverage with respect to the other years (2007-2010).

Atmos. Chem. Phys. Discuss., https://doi.org/10.5194/acp-2018-589
Manuscript under review for journal Atmos. Chem. Phys.
Discussion started: 24 August 2018

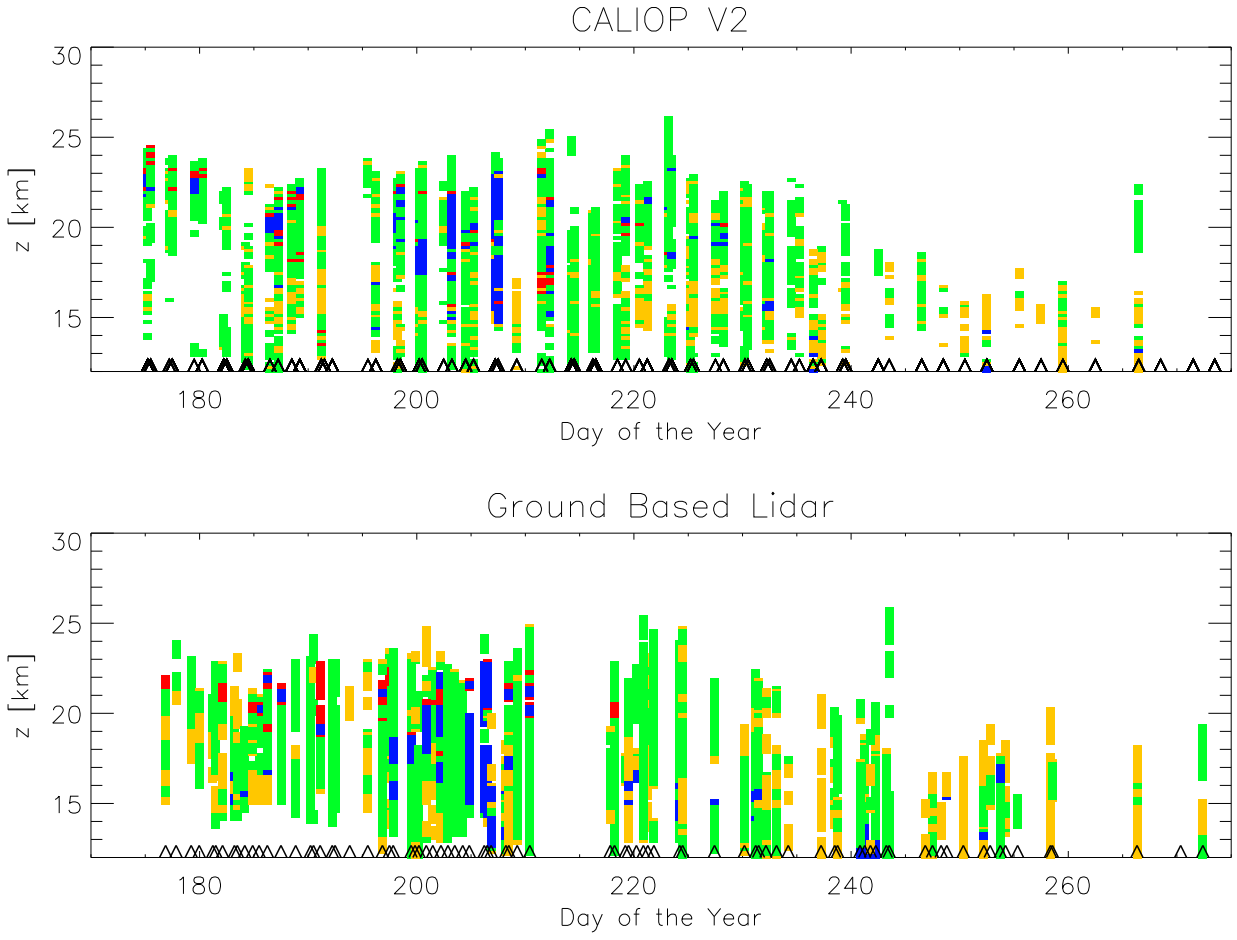

Figure 1. PSC observations recorded in 2006 above McMurdo. Upper panel: CALIOP around McMurdo from V2 product. Lower panel: Ground-based lidar data. The PSC classes are represented by colors; green = NAT mixtures, orange = STS, blue = ice, red = enhanced NAT mixtures. Triangles on the x-axis indicate the day when at least one observation was available.

Both the CALIOP PSC product, and the classification of the ground-based lidar optical parameters, classified with the V2 algorithm adapted for ground-based data, provide a similar view for this winter with a dominance of NAT mixtures with isolated periods of ice PSCs at the core of the PSC winter season. Enhanced NAT mixtures appear jointly to ice clouds while STS are observed in the lower layers at the beginning and at the end of the season. These results are not directly comparable with the analysis previously reported (Di Liberto et al., 2014), where a more classical classification scheme for ground-based data was adopted and different PSC classes were assigned. Although the overall agreement with CALIOP is rather good, many small differences are evident, and confirm that a point-to-point comparison of these data is not straightforward.

For this reason a statistical comparison, including five years of measurements (2006-2010) has been pursued.

Atmos. Chem. Phys. Discuss., https://doi.org/10.5194/acp-2018-589
Manuscript under review for journal Atmos. Chem. Phys.
Discussion started: 24 August 2018

Atmospheric Chemistry and Physics Discussions

PSC classes	McMurdo ground-based [%]	McMurdo CALIOP [%]
STS	25.5	24.2
NAT mixtures	59.4	57.9
enhanced NAT mixtures	1.5	2.6
ice	13.6	15.3

Table 1. Frequency of occurrence (in %) of PSCclasses during June-July-August-September between 12 and 30 km height. The ice-class for CALIOP includes also mountain wave ice.

Table 1 shows the relative abundance of occurrences for all four PSC classes as classified by CALIOP and ground-based lidar. Overall there is a very good agreement for ice and STS, while for the ground-based lidar there is a small shift from enhanced NAT mixtures to NAT mixtures with respect to CALIOP. We should bear in mind, however, that this agreement, in terms of occurrences of the different PSC classes in a five year period at McMurdo, might be in part fortuitous, since significant differences might exist during the winter season and also as a function of altitude. In order to explore these possible differences, we firstly compare the PSC occurrences as a function of altitude during the winter season, by accumulating all PSC observations for the five year period (2006-2010) for each month (June through September) between 12 and 30 km. In figure 2 the vertical profiles of monthly PSC occurrence for the years 2006-2010 are reported. Occurrence is calculated as the fraction of observations where a determined class of PSC occurs. The upper row displays the CALIOP PSC product, while the lower row shows the PSC classification obtained by applying the approximate algorithm to the ground-based data.

Atmos. Chem. Phys. Discuss., https://doi.org/10.5194/acp-2018-589
Manuscript under review for journal Atmos. Chem. Phys.
Discussion started: 24 August 2018

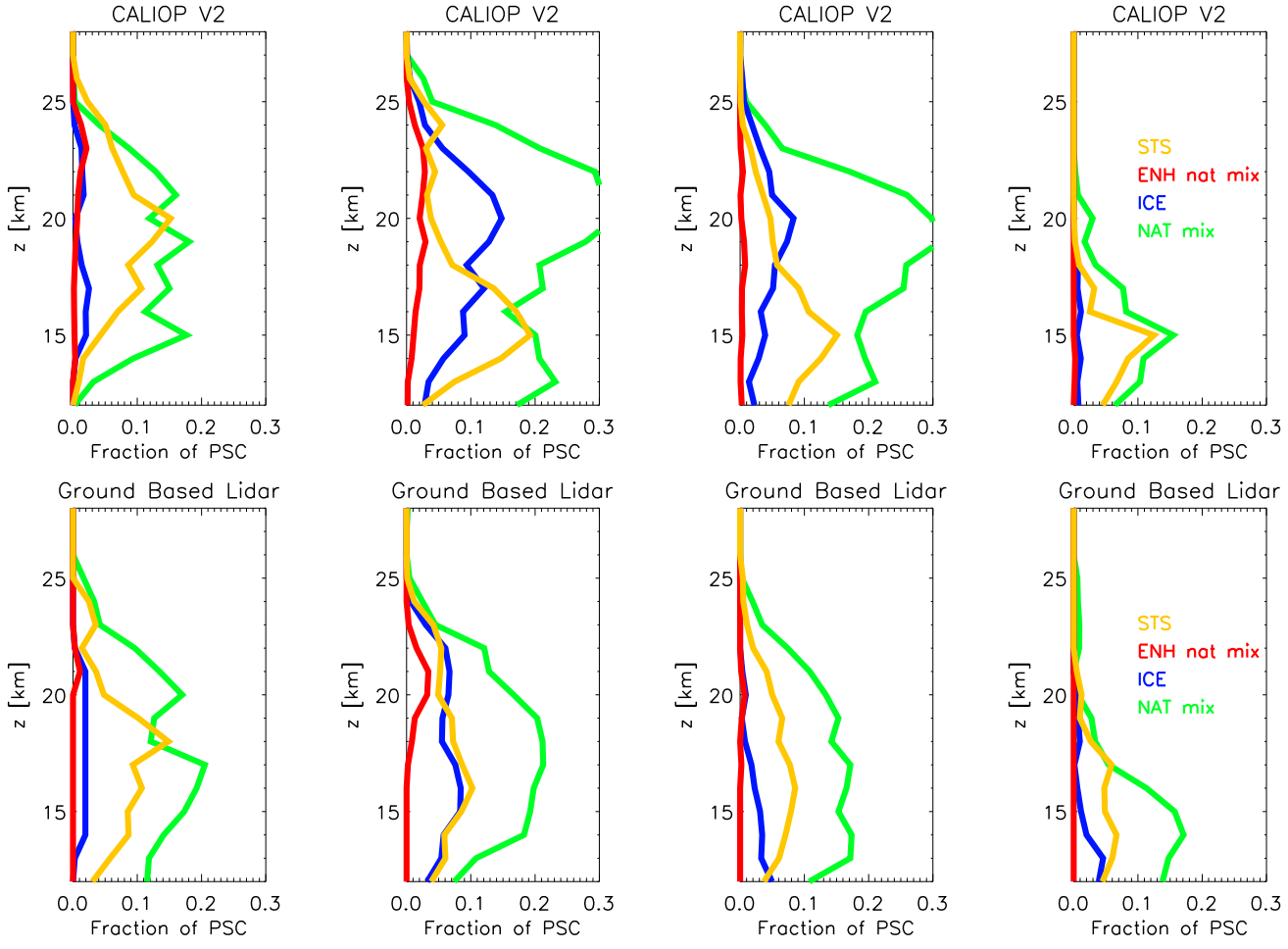

Figure 2. Winter 2006-2010 PSC vertical distribution as a fraction of the total observations for the four PSC classes (orange = STS, green = NAT mixtures, red = enhanced NAT mixtures, blue = ice), the four columns indicate the months June to September (from left to right). Upper row: CALIOP V2 product. Lower row: ground-based lidar at McMurdo.

The figure shows that PSCs are observed up to 25 km in June, July and August, while they are descending below 20 km in September. Above 25 km the number of PSC observations is negligible, both for ground-based and CALIOP observations. There is a reasonable agreement between CALIOP and ground-based observations for ice, enhanced NAT mixtures and STS. NAT mixtures are the dominating species during the winter, with a slightly different altitude ditribution in July and August; CALIOP observations show a maximum for NAT mixtures around 20 km, while the ground-based data show a flatter distribution. Ice and enhanced NAT mixtures occur mainly in July, the enhanced NAT mixtures are observed between 17 and 25 km, while ice persists also at lower altitudes. The overall agreement is satisfactory however, considering the different observation geometries and statistics. The main discrepancies appear at lower altitudes, where the ground-based lidar observes more ice in most months with respect to CALIOP, and also the vertical distribution of NAT is more shifted to lower altitudes wrt

Atmos. Chem. Phys. Discuss., https://doi.org/10.5194/acp-2018-589
Manuscript under review for journal Atmos. Chem. Phys.
Discussion started: 24 August 2018

Atmospheric Chemistry and Physics Discussions

CALIOP. Another way to compare the statistical distribution of PSCs as observed by both instruments is to use the temperature dependence. The temperature dependence of the occurrence of different PSC classes has been studied intensively with in-situ and remote data with the goal to to confirm hypotheses on microphysical mechanisms of PSC formation (Peter, 1997). In this context we want to use it as another tool to investigate a possible bias when comparing ground-based and satellite based observations centered on McMurdo. The temperature data base used for the data analysis of CALIOP is MERRA-2 (Modern Era Retrospective analysis for Research and Applications) which uses the GEOS-5 analysis. In a previous analysis of the McMurdo ground-based lidar data (Di Liberto et al., 2014), the temperature was obtained from radiosoundings and, where these were not available, from NCEP. For the present analysis, however, we choose to use the same MERRA-2 temperature data for the ground-based data, in order to avoid a temperature bias while comparing with CALIOP data. The ice formation temperature T_{ice} has been obtained from daily values of the EOS MLS retrieved data for H_2O number densities.

The probability density functions of the different species are reported in figure 3 as the ratio of the occurrence of each species and the total number of observations at the specific temperature T-T_{NAT}. The total number of observations is reported as well, in arbitrary units, to indicate the variation of the number of observations with temperature. The ratio of occurrence has not been displayed when the number of observations at a specific temperature is too low to be statistically valid (less than 5 % of the total observations.

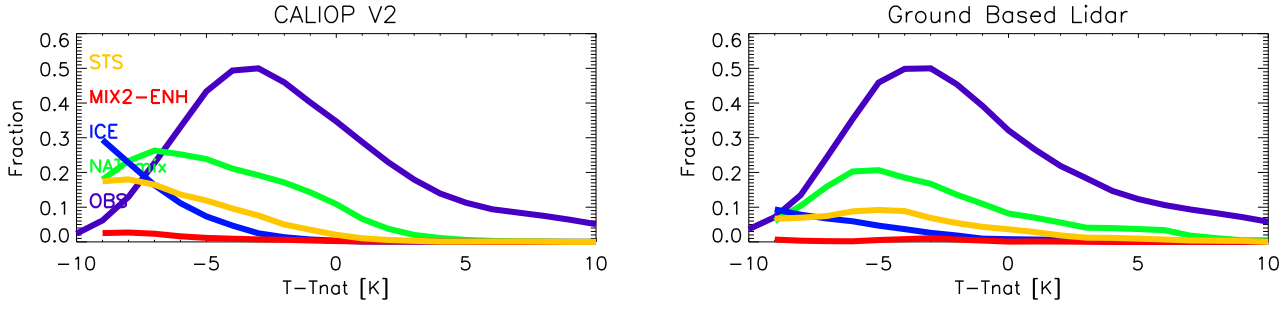

Figure 3. Fraction of PSC observations in 2006-2010 centered at McMurdo (calculated as the ratio of the number of data points for each PSC class and the total number of data points) as a function of the difference between the temperature and the equilibrium temperature for NAT. PSC classes are reported in different colors. The purple line indicates the total number of observations at a specific temperature in arbitrary units.

One can observe that the relative number of occurrences as observed by spaceborne and ground-based lidar at McMurdo vary in a similar way with the local temperature. The total number of observations have a very similar temperature distribution, which indicates that the two instruments statistically sample air masses with a similar temperature distribution. The temperature dependence of the NAT and STS PSCs is very similar, although the peak for NAT is slightly shifted to lower temperatures. The onset for ice is the same, although it appears to be more present at lower temperatures for CALIOP with respect to the ground-based data. This is probably due to the fact that ice is not frequently observed around McMurdo (Adriani et al., 2004; Di Liberto et al., 2014) and that the few observations occur at different altitudes as can be seen also in figure 2.

Atmos. Chem. Phys. Discuss., https://doi.org/10.5194/acp-2018-589
Manuscript under review for journal Atmos. Chem. Phys.
Discussion started: 24 August 2018

Atmospheric Chemistry and Physics Discussions

As a conclusion, the statistical agreement between CALIOP and ground-based data is rather good above 15 km, and is biased below, probably due to a a different rejection of isolated PSC observations as performed with a different spatial coherence criterion.

3 Comparison of CALIOP PSC observations in the Southern Hemisphere with CCM simulations

The coupling of stratospheric chemical models with climate models has led to a new generation of models. These coupled Chemistry-Climate Models (CCMs) are used within the Chemistry-Climate Model Validation activity 2 (CCMVal-2) [Eyring et al., 2008] and represent both stratospheric chemistry and atmospheric climate. CCMVal-2 models do not include a representation of stratospheric aerosol physics and chemistry, but use parametrizations to take into account the formation of PSCs. There are large differences among CCMs for their treatments, regarding their formation mechanisms, types, and sizes (Morgenstern et al., 2010). All CCMs involved in the CCMVal-2 experiment include water-ice PSCs; all except CMAM also include $HNO_3 \cdot 3\ H_2O$ (nitric acid trihydrate, NAT). Most CCMs furthermore treat sulfate aerosols, e.g. in the form of supercooled ternary solutions (STS) of sulfuric acid (H_2SO_4), nitric acid (HNO_3), and water (Morgenstern et al., 2010).

Evaluating the ability of CCMs to reproduce ice and NAT PSCs is a key factor to interpret simulated stratospheric polar ozone changes. The comparison of space-borne PSC observations with CCM simulations requires adequate diagnostical methods. Here we assess the ability of models to simulate PSCs taking into account diagnostics that mostly focus on microphysical factors, such as the NAT and ice surface area densities and diagnostics that are sensitive to the coupling of those with the simulation of polar vortex variability and its mean state.

3.1 Overview of the models

Here we consider 4 CCMs involved in the CCMVal-2 experiment , CAM3.5 (Community Atmosphere Model 3.5) and WACCM (Whole-Atmosphere Chemistry-Climate Model) both developed at NCAR, CCSRNIES (Center for Climate System Research/National Institute for Environmental Studies, Japan), and LMDZrepro (Laboratoire de Météorologie Dynamique Zoom- REPROBUS), developed at IPSL, and one CCM included in the Chemistry–Climate Model Initiative (CCMI), WACCM-CCMI.

Some general features such as the horizontal resolution and vertical levels have been displayed in Table 2.

Atmos. Chem. Phys. Discuss., https://doi.org/10.5194/acp-2018-589
Manuscript under review for journal Atmos. Chem. Phys.
Discussion started: 24 August 2018

Atmospheric Chemistry and Physics Discussions

CCM	Years	Horizontal resolution	vertical grid	References
CAM3.5	1991-1999	2.5^o x 1.9^o	L26	Lamarque et al. (2008)
CCSRNIES	1991-2005	2.8^o x 2.8^o	L34	Akiyoshi et al. (2009)
LMDZrepro	1991-2005	3.75^o x 2.5^o	L50	Jourdain et al. (2008)
WACCM	1995-2005	2.5^o x 1.9^o	L66	Garcia et al. (2007)
WACCM-CMMI	1960-2010	2.5^o x 1.9^o	L66/88	Solomon et al. (2015); Garcia et al. (2017)

Table 2. Horizontal resolution and number of levels for the CCMs used. The output of the models has been taken for the years indicated in the second column.

All models include water-ice PSCs as well as nitric-acid-trihydrate (NAT). They also treat sulfate aerosols in different forms, such as supercooled ternary solutions of sulfuric acid, water and nitric acid (STS) (CAM3.5, WACCM and CCSRNIES), or liquid aerosol (LMDZrepro).

The conditions at which PSCs condense and evaporate vary, not only for water-ice PSCs but also for NAT and STS, between CCMs (Morgenstern et al., 2010). The simplest assumption is that PSCs are formed at the saturation points of HNO_3 over NAT and H_2O over water-ice. This assumption is made in most CCMVal-2 CCMs.

The microphysical processes of condensation and evaporation of the PSCs vary among the different models. Most models use a thermodynamical equilibrium assumption that PSCs are formed at the saturation conditions for nitric acid over NAT and water over ice. CAM3.5 and WACCM allow for saturation of up to 10 times saturation (Morgenstern et al., 2010). Table 3 illustrates how the CCMs considered here use different formation processes and sedimentation velocities.

CCM	Thermodynamics	particles	Sedimentation
CAM3.5	EQ	NAT/ice/STS	NAT / ice but not STS
CCSRNIES	EQ	NAT/ice/STS	NAT/ice dep. on mode radius
LMDZrepro	EQ	NAT/iice/LA	
WACCM	NAT: HY; ice:EQ	NAT/ice/STS	NAT / ice but not STS
WACCM-CMMI	NAT: HY; ice:EQ	NAT/ice/STS	NAT / ice but not STS

Table 3. Main features of simulation and of the microphysics of polar stratospheric clouds. EQ =thermodynamic equilibrium with gaseous HNO3 / H2SO4 / H2O assumed. HY = non-equilibrium / hysteresis considered. LA=liquid aerosol, SAD = sulphuric acid dihydrate (adapted from CCMVal-2 report (2010)).

Note that the equilibrium assumption allows to determine the total mass of condensed PSCs, and that a size distribution needs to be postulated in order to derive surface area densities (SAD). Since the sedimentation velocity depends on the size

of the particles, the size distribution assumed has a significant impact on denitrification and dehydration processes through sedimentation of PSCs.

Some differences between WACCM and WACCM-CCMI should be mentioned here. While the CCMVal-2 version of WACCM simulated Southern Hemisphere winter and spring temperatures that were too cold compared with observations, in the CCMI-1 simulations this problem was addressed by introducing additional mechanical forcing of the circulation via parameterized gravity waves(Garcia et al., 2017). Also the polar heterogeneous chemistry was recently updated (Wegner et al., 2013) and further evaluated by (Solomon et al., 2015).

Recently Zhu and co-workers introduced a new PSC model (Zhu et al., 2017b, a, 2015) within the CESM1 Whole Atmosphere Community Climate Model version 4.0 (WACCM 4.0), with Specified Dynamics (SD) coupled with the Community Aerosol and Radiation Model for Atmospheres (CARMA) model. This new model takes into account detailed microphysical processes for the formation of NAT and STS, instead of the parametrizations used in the CCMVal-2 and CCMI-1 models. An evaluation study on EMAC has been reported (Khosrawi et al., 2018), using MSBM for the processes related to PSCS (Kirner et al., 2011). The submodel MSBM uses two parametrizations for the NAT formation, one based on the heterogeneous formation on ice, the second for the homogeneous formation of NAT. The model simulations for the Arctic winter 2009/2010 and 2010/2011 showed that simulated PSC volumes are smaller than those observed and that the simulations do not produce PSCs as high as they are observed.

Here we limit our analysis to simulations produced by four models from CCMVal-2 and one model from CCM1. One of the goals is to use different diagnostics to test the model simulations versus the CALIOP observations. Recent studies of problems in simulating PSCs can be found in (Brakebusch et al., 2013; Wegner et al., 2013; Zhu et al., 2015, 2017a).

3.2 Comparison based on the PSC vertical extent

Presently, the evaluation of CCMs for what concerns stratospheric aerosol and in particular PSCs is still incomplete. The SPARC report (Eyring et al., 2010) includes a model inter-comparison of PSC surface area densities (SAD) concluding that more work is needed to evaluate NAT and ice aerosols and that a comparison with observations is clearly needed, since currently no global data sets that can be used to evaluate these constituents, are available. The CCMVal-2 data base includes the surface area density (SAD) for NAT and ice clouds and sulphates. Here we restrict the analysis to the reference simulations (REF-B2), the transient set of simulations aiming at reproducing the past 1960-2006 conditions where all forcings are taken from observations (Eyring et al., 2010).)

Both model and CALIPSO observations in the latitude range [83^o,60^o] are binned in a 3.5^ox7^o grid and on 15 vertical levels with a resolution of 1.5 km. CCMVal-2 data south of 83^oS are excluded to fit with CALIPSO latitudinal coverage. In this study, we use two different WACCM versions, with the same PSC scheme, used within CCMVal-2 and CCMI.

To be able to compare with the CALIOP lidar observations, we have to derive the mean PSC layer vertical extent and the frequency of occurrence as a function of height and of temperature for the models from the PSC surface area density (SAD) spatial distribution. To do so, it is necessary to apply a simplified observation operator to the model output (i.e. identify the model grid points where a lidar would have observed NAT or ice clouds by defining a threshold for the SAD values produced

Atmos. Chem. Phys. Discuss., https://doi.org/10.5194/acp-2018-589
Manuscript under review for journal Atmos. Chem. Phys.
Discussion started: 24 August 2018

Atmospheric Chemistry and Physics Discussions

by the models). We firstly define a vertical extent of PSCs as the sum of all layers containing a specific class of PSC. In order to study seasonal and geographical variations, we construct maps of monthly means by accumulating all observations from 2006 to 2010. Figure 4 shows maps of the monthly mean vertical extent (in km) for ice, NAT mixtures, enhanced NAT mixtures and STS PSCs as observed by CALIOP from 2006 to 2010.

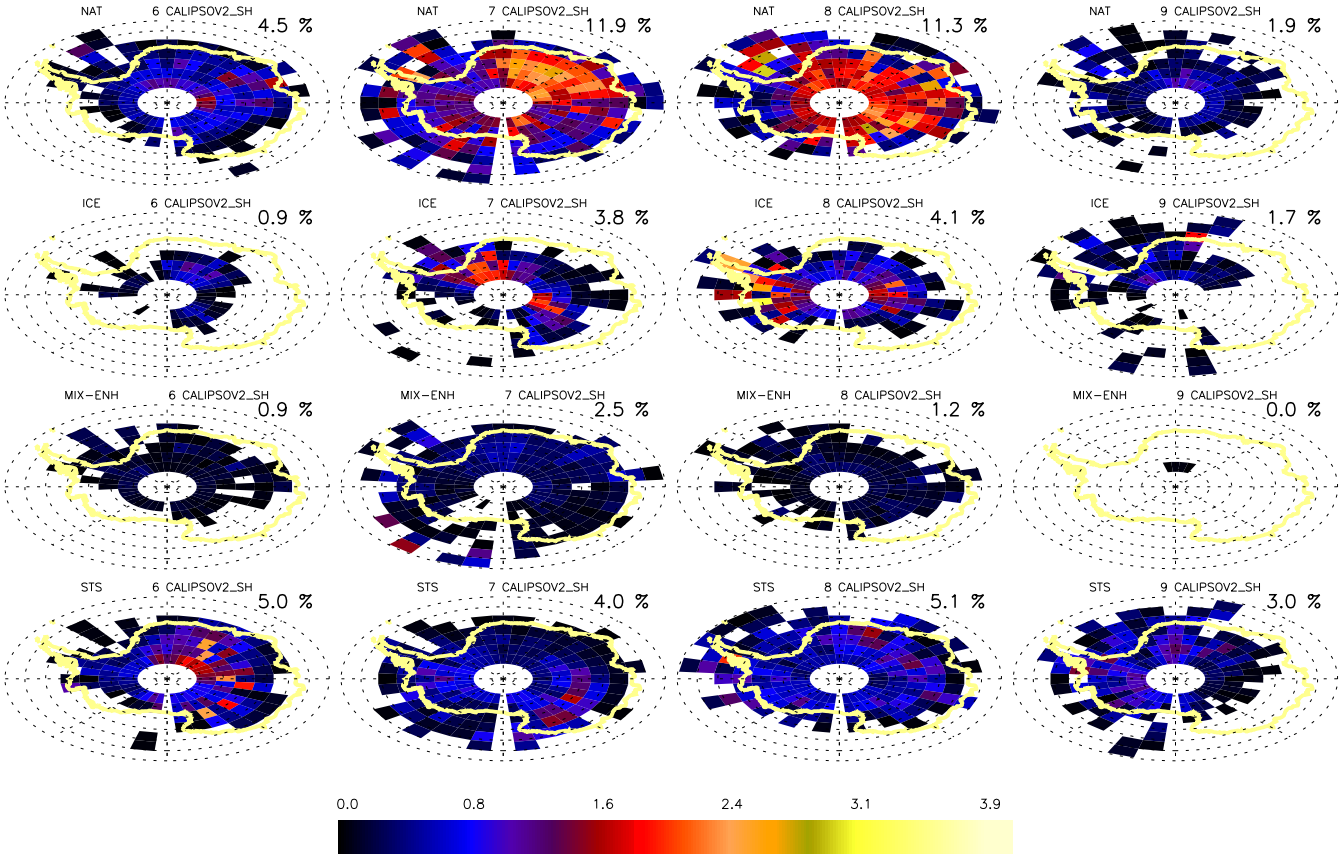

Figure 4. The vertical extent for NAT mixtures, ice, enhanced NAT mixtures and STS (from top to bottom) obtained from CALIOP observations, averaged over 5 years for June, July, August, September (left to right). The fraction of the overall air volume (between 12 and 30 km height south of 60^{o}S) occupied by different PSC classes for each month is reported in the top right corner. The colour scale indicates the number of km occupied by PSCs between 12 and 30 km

The ice PSC distribution has a clear non-zonal longitudinal distribution with a maximum in the 90^o - 0^o longitude sector. This appears as a clear indication that mountain waves play a major role in ice cloud formation on the lee side of the Transantarctic chain (that crosses the continent as an ideal prolongation of the Antarctic Peninsula). This has previously been reported by Noel et al. (2009) and by Alexander et al. (2011) based on the combination of CALIPSO and COSMIC GPS-RO data. The latter

Atmos. Chem. Phys. Discuss., https://doi.org/10.5194/acp-2018-589
Manuscript under review for journal Atmos. Chem. Phys.
Discussion started: 24 August 2018

Atmospheric Chemistry and Physics Discussions

reports an analysis based on a single winter data set showing that mountain wave generation is a regular feature influencing ice PSC distribution. NAT-like PSCs have a maximum in the 0^o90^o longitude quadrant. Höpfner et al. (2006) suggested that mountain waves may be responsible for the non-zonal NAT distribution that were indeed observed closer to the Transantarctic chain while Alexander et al. (2011) also consider that NAT formation can be related to the outflow of ice clouds. Wang et al. (2008) pointed out that increased convection due to orographic triggering in the lee of the Transantarctic chain is related to the occurrence of enhanced NAT mixtures. Enhanced NAT mixtures have a minor vertical extent with respect to NAT mixtures and form in the inner vortex (where colder temperatures occur) with a zonal distribution similar to NAT mixtures. STS are observed predominantly in June, again with a clear majority in the same region of NAT and enhanced NAT mixtures formation. The McMurdo site is characterized by a majority of NAT-like PSCs (also visible in the time-series reported in figure 1).

Here we compare maps of NAT and ice PSC occurrences, produced by the two WACCM models, showing the geographical distribution of NAT and ice in the southern hemisphere (south of 60^oS) for the winter season, from June to September. (see figures 5 and 6) with CALIOP observations (figure 4).

The first one is sufficiently representative of the bias observed in all CCMVal-2 simulations analyzed here. The second simulation is shown to give a qualitative indication of the improvement of PSC distribution with a more reliable temperature and Antarctic stratosphere dynamics. The vertical extent for the models is estimated analogously to the observations. The horizontal resolution applied to estimate the occurrence is the same among models and CALIOP data. Effect of vertical resolution differences between model and observations is reduced by estimating a total aggregate vertical occurrence.

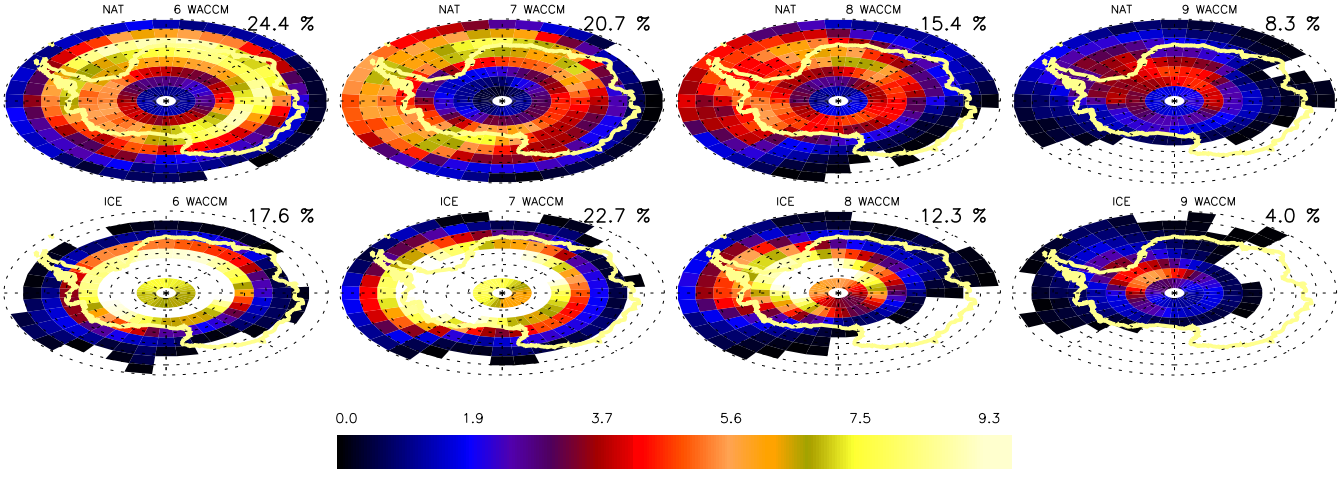

Figure 5. WACCM PSCs vertical extent for NAT and ice, averaged over five years during the months of June, July, August, September (left to right). Please note that the color scale is different from figures 4 and 6. The fraction of the overall air volume (between 12 and 30 km height south of 60^oS) occupied by different PSC classes for each month is reported in the top right corner.

Atmos. Chem. Phys. Discuss., https://doi.org/10.5194/acp-2018-589
Manuscript under review for journal Atmos. Chem. Phys.
Discussion started: 24 August 2018

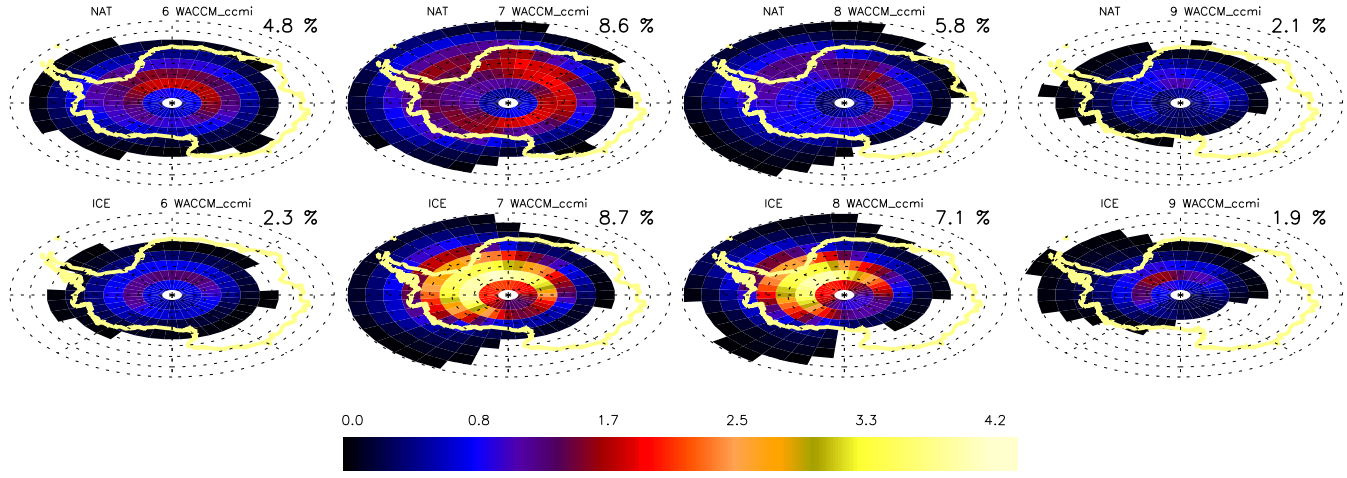

Figure 6. WACCM-CCMI PSCs vertical extent for NAT and ice, averaged over five years during the months of June, July, August, September (left to right). Please note that the color scale is different from figures 4 and 5. The fraction of the overall air volume (between 12 and 30 km height south of 60^{o}S) occupied by different PSC classes for each month is reported in the top right corner.

Several differences are evident. First of all the geographical distribution of the PSCs in the simulations appears to be different from the CALIOP observations, although the small numbers of observations, in particular for ice in June and September makes any comparisons with models speculative. The NAT occurrences as observed by CALIOP in July and August are mainly concentrated in East Antarctica, while WACCM predicts more NAT towards the Antarctic peninsula and the Weddell Sea. The WACCM model shows too large occurrences of both NAT and ice PSCs with respect to the the more recent WACCM-CMMI model and with respect to observations. The onset of PSCs as predicted by the models is also anticipated with respect to observations. The WACCM-CMMI model compares better with observations, for what concerns the seasonal behaviour, the occurrences and geographical distribution. The reduction of the cold bias in the WACCM-CCMI version (Doug Kinnison personal communication) may be the most relevant factor leading to PSC distribution improvement in the new model version.

Atmos. Chem. Phys. Discuss., https://doi.org/10.5194/acp-2018-589
Manuscript under review for journal Atmos. Chem. Phys.
Discussion started: 24 August 2018

Atmospheric Chemistry and Physics Discussions

	NAT mixtures				ice			
	Jun	July	Aug	Sep	Jun	July	Aug	Sept
CALIPSO*	4.5	11.9	11.3	1.9	0.9	3.8	4.1	1.7
CAM3.5	25.9	26.0	22.8	10.1	23.1	28.5	16.1	1.9
CCSRNIES	14.9	36.8	38.6	20.2		17.3	23.2	8.9
LMDZrepro	2.0	5.9	14.4	17.8		1.2	1.9	
WACCM	24.4	20.7	15.4	8.3	17.6	22.7	12.3	4.0
WACCM-cmmi	4.8	5.6	5.8	2.1	2.3	8.7	7.1	1.9

Table 4. Total PSC frequencies (in %) in the 13-25 km height layer for NAT and ice clouds for June-July- August-September for the observations and models. Fractions below 1% are not reported in the table. Note that CALIPSO NAT includes the enhanced NAT mixtures class

Table 4 reports the total PSC vertically integrated frequencies of occurrence for the five models and for CALIPSO over June to September. Models in general significantly overestimate PSCs in June with respect to observations, as confirmed by the CCMVal report (2010) showing a high occurrence from May onward with a maximum often occurring in June. The LMDZ model is a clear outlier with a very large underestimation of both NAT and ice PSCs all throughout the season. The largest biases are found for ice PSCs that tend to be significantly overestimated.

3.3 Comparison based on SAD

Another diagnostic method consists of comparing the surface area density (SAD) for CCMs and CALIOP. A range of SAD values can be obtained for NAT and ice for each model. Surface area density for the CCMVal-2 is estimated based on a semi-empirical relation between mass and mean surface areas given to the model providers and reported in the CCMVal-2 report. We must be aware, however, that SAD is a derived variable and depends on the assumptions on the mean particle size for each model (as detailed in the CCMVAl-2 report, 2010). When models predict both NAT and ice clouds, we assigned the SAD to ice if the SAD for ice is larger by a factor of 3 than the one for NAT. The SADs for CALIOP have been evaluated by using an empirical relationship derived from coincident lidar and size distributions observations (Snels et al., 2018). Figure 7 shows the histograms of ice and NAT values for SAD for each model together with the range of SAD reported in (Adriani et al., 1995). The fraction is normalized to the total number of model grid points in order to identify the differences in PSC occurrence among models and between classes.

Atmos. Chem. Phys. Discuss., https://doi.org/10.5194/acp-2018-589
Manuscript under review for journal Atmos. Chem. Phys.
Discussion started: 24 August 2018

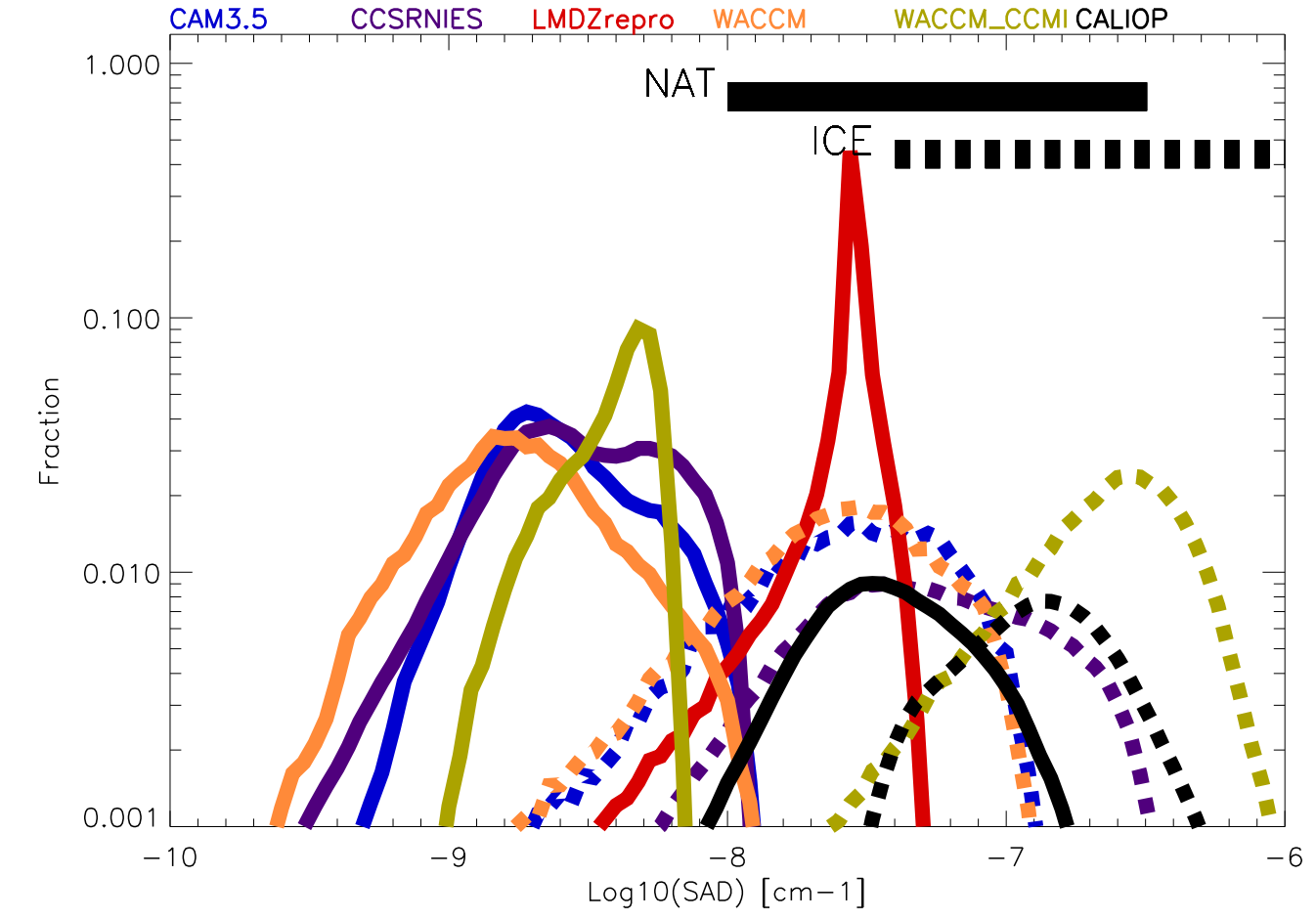

Figure 7. Histogram of the NAT (solid lines) and ice (dashed lines) Surface Area Densities for some CCMVal models and for CALIOP are displayed. The histograms for the model data have been truncated and represent 93% of the total SAD. The straight lines at the top of the figure indicate the range of SAD values for NAT and ice "observed" by ground-based lidars and are taken from (Adriani et al., 1995).

We observe that for most of the models NAT PSCs have SAD ranging between $3{\cdot}10^{-10}$ and 10^{-8} cm^{-1} except for LMDZrepro that has larger SAD for NAT PSCs and is clearly an outlier. In general all models produce SADs for NAT that are smaller by one order of magnitude than the SAD calculated from CALIOP data, except for LMDZ-repro. The variability among models for the NAT SAD may be related to the assumptions made on the number of particles per cm^{-3}. The narrow peak at larger NAT SAD values for the LMDz model could be consistent with the use of much larger particle number density and smaller particle radius in the simulation. This in turn would give less irreversible denitrification processes simulated by the models with larger NAT SAD (CCMVAl-2 report, 2010, Chapter 6). Most of the models have ice PSCs in a SAD range between $2{\cdot}10^{-9}$ and 10^{-6} cm^{-1} and are generally a factor of 2-3 smaller than CALIOP values, except for the WACCM-CCMI simulations, which predict a larger value than that derived from CALIOP observations.

Atmos. Chem. Phys. Discuss., https://doi.org/10.5194/acp-2018-589
Manuscript under review for journal Atmos. Chem. Phys.
Discussion started: 24 August 2018

Atmospheric Chemistry and Physics Discussions

3.4 Comparison based on PSC occurrences

The comparison between CALIOP and CCMs can also be made by using the occurrences as a function of T-T_{NAT}, similarly to what has been done above for the comparison between ground-based and satellite-borne lidars above McMurdo. In figure 8 the PSC occurrences as predicted by the models and as observed by CALIPSO between 60^{o}S and 83^{o}S averaged over the 2006-2010 period have been displayed as a function of T-T_{NAT}, where T_{NAT} has been calculated from HNO_3 and H_2O number densities. Note that the models produce only NAT and ice occurrences.

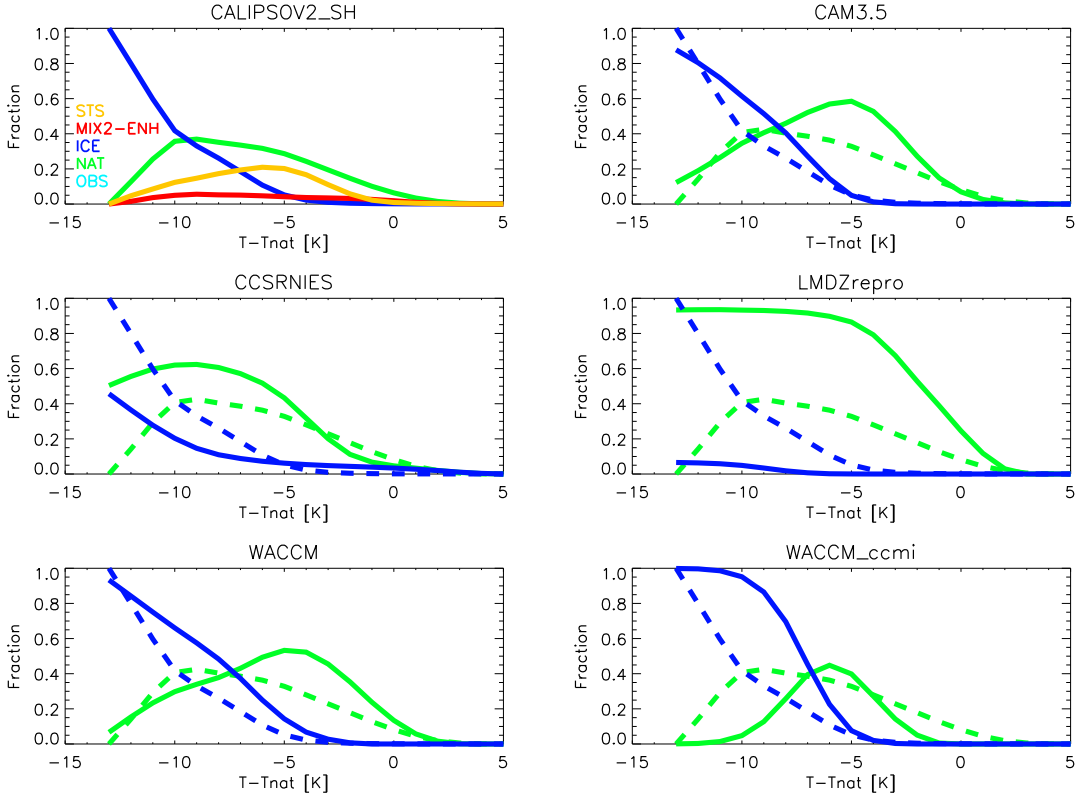

Figure 8. As Figure 3 but for 60-83^{o}S CALIOP V2 observations and CCMs data. CALIOP data are reported as dashed lines on each model as reference.

As reported in the CCMVal-2 report, most models show a well-known cold pole bias in stratospheric temperature. The bias is in general attributed to model dynamics, as in (Austin et al., 2003) that identifies a lack of westward wave forcing resulting in a more intense and persistent polar vortex. A clear improvement is in fact obtained with an improvement in the gravity waves scheme as in (Kinnison et al., 2007), resulting in more realistic temperatures in the WACCM-CCMI simulation as described above.

Atmos. Chem. Phys. Discuss., https://doi.org/10.5194/acp-2018-589
Manuscript under review for journal Atmos. Chem. Phys.
Discussion started: 24 August 2018

Atmospheric Chemistry and Physics Discussions

The onset for NAT is similar for all models, except for WACCM-cmmi, where no NAT is observed above T_{NAT}. The onset for ice is occurring for T-T_{NAT} = -5 K for all models, except for CCSRNIES. LMDZ-repro has a too slow formation for ice and a too fast formation for NAT. The family CAM3.5, WACCM and WACCM-CCMI all have a too fast progression for ice and for NAT.

The fraction of data with different PSC classes helps in evaluating how realistic the microphysical scheme is, since this variable is normalized to the number of observations and in principle independent from the possible biases. CALIPSO sees a progressive increase of the fraction with temperature decreasing and an increase of ice PSC with T-T_{NAT} < -5 K that is close to the ice formation temperature. The total fraction of ice PSCs increases steadily from temperatures below T_{NAT} reaching 0.8 at T-T_{NAT}=-12 K. In general all models (except LMDZrepro) show a sharper increase of the fraction at T-T_{NAT} < -5 K with respect to CALIPSO but with different partitioning between NAT and ice. LMDZrepro shows an unrealistically low ice content, while the for other models ice is dominant for low temperatures.

In general CAM3.5 and WACCM that share the same microphysical scheme have a more than satisfactory agreement, notwithstanding the cold bias that generates an excessive PSC coverage. On the other hand, WACCM-CCMI has a more realistic PSC coverage but a likely too efficient ice PSC generation due to the new scheme. So, even if the overall skills f the model are largely improved, this kind of diagnostics (the slopes of curves in figure 8 and the "onset" PSC temperature) suggest the need to explore the ability of single component of the model system such as the microphysical scheme.

4 Conclusions

A statistical comparison has been made of five years of PSC observations at McMurdo, obtained from ground-based and satellite-borne lidar measurements. The analysis of the ground-based data has been performed by using a detection and classification algorithm which closely follows the V2 algorithm applied to CALIOP data, in order to avoid a bias due to different classification schemes. In favorable circumstances, however, a point-to-point comparison of ground-based and satellite-borne lidar observations is feasible, as can be seen in figure 1. The relative occurrences of the four PSC classes, STS, NAT mixtures, enhanced NAT mixtures and ice, averaged over five years are very similar for ground-based and CALIOP observations. The vertical distribution and the temperature dependence of the occurrences of the different PSC classes show some discrepancies, in particular below 15 km. As a conclusion, the statistical agreement between CALIOP and ground-based data is rather good above 15 km, and is biased below, probably due to a a different rejection of isolated PSC observations as performed with a different spatial coherence criterion.

From CALIOP data we have derived a set of diagnostics, useful to evaluate if biases in Chemistry Climate Models are related to their PSCs microphysical schemes. The diagnostics are based on spatial (vertical and horizontal) SAD distribution of ice and NAT particles together with their temperature distributions. Those diagnostics are here applied to a subset of CCM simulations form CCMVal2 and to a more recent version of WACCM from CCMI. Models fail to reproduce realistic geographical distributions of PSCs within the polar vortex. Moreover the model SADs are generally lower than those observed for NAT and

show a too efficient PSC production at low temperatures. While these discrepancies are evident for the older models, the more recent WACCM-CCMI model compares better with CALIOP observations for ice and NAT.

Acknowledgements. The authors acknowledge the financial support by PNRA in the frame work of the projects 2004/2.09 and 2009/B.08. We also acknowledge the support of the ISSI-PSC initiative project. Logistical and winter-time technical support was provided by the US National Science Foundation through NSF awards 0538679 and 0839124 to the University of Wyoming.

References

Achtert, P. and Tesche, M.: Assessing lidar-based classification schemes for polar stratospheric clouds based on 16 years of measurements at Esrange, Sweden, Journal of Geophysical Research: Atmospheres, 119, 1386–1405, doi:10.1002/2013JD020355, 2014.

Adriani, A., Deshler, T., Gobbi, G. P., Johnson, B. J., and Di Donfrancesco, G.: Polar stratospheric clouds over McMurdo, Antarctica, during the 1991 spring: Lidar and particle counter measurements, Geophysical Research Letters, 19, 1755–1758, doi:10.1029/92GL01941, 1992.

Adriani, A., Deshler, T., Di Donfrancesco, G., and Gobbi, G.: Polar stratospheric clouds and volcanic aerosol during spring 1992 over McMurdo Station, Antarctica: Lidar and particle counter comparative measurements, Journal of Geophysical Research-Atmospheres, 100, 25 877–25 897, 1995.

Adriani, A., Massoli, P., Di Donfrancesco, G., Cairo, F., Moriconi, M., and Snels, M.: Climatology of polar stratospheric clouds based on lidar observations from 1993 to 2001 over McMurdo Station, Antarctica, Journal of Geophysical Research-Atmospheres, 109, doi:10.1029/2004JD004800, 2004.

Akiyoshi, H., Zhou, L. B., Yamashita, Y., Sakamoto, K., Yoshiki, M., Nagashima, T., Takahashi, M., Kurokawa, J., Takigawa, M., and Imamura, T.: A CCM simulation of the breakup of the Antarctic polar vortex in the years 1980-2010 under the CCMVal scenarios, Journal of Geophysical Research: Atmospheres, 114, n/a–n/a, doi:10.1029/2007JD009261, d03103, 2009.

Alexander, S. P., Klekociuk, A. R., Pitts, M. C., McDonald, A. J., and Arevalo-Torres, A.: The effect of orographic gravity waves on Antarctic polar stratospheric cloud occurrence and composition, Journal of Geophysical Research-Atmospheres, 116, doi:10.1029/2010JD015184, 2011.

Austin, J., Shindell, D., Beagley, S. R., Brühl, C., Dameris, M., Manzini, E., Nagashima, T., Newman, P., Pawson, S., Pitari, G., Rozanov, E., Schnadt, C., and Shepherd, T. G.: Uncertainties and assessments of chemistry-climate models of the stratosphere, Atmospheric Chemistry and Physics, 3, 1–27, doi:10.5194/acp-3-1-2003, https://www.atmos-chem-phys.net/3/1/2003/, 2003.

Brakebusch, M., Randall, C. E., Kinnison, D. E., Tilmes, S., Santee, M. L., and Manney, G. L.: Evaluation of Whole Atmosphere Community Climate Model simulations of ozone during Arctic winter 2004–2005, Journal of Geophysical Research: Atmospheres, 118, 2673–2688, doi:10.1002/jgrd.50226, http:https://doi.org/10.1002/jgrd.50226, 2013.

Browell, E. V., Butler, C. F., Ismail, S., Robinette, P. A., Carter, A. F., Higdon, N. S., Toon, O. B., Schoeberl, M. R., and Tuck, A. F.: Airborne lidar observations in the wintertime Arctic stratosphere: Polar stratospheric clouds, Geophysical Research Letters, 17, 385–388, doi:10.1029/GL017i004p00385, 1990.

Cairo, F., Donfrancesco, G. D., Adriani, A., Pulvirenti, L., and Fierli, F.: Comparison of various linear depolarization parameters measured by lidar, Appl. Opt., 38, 4425–4432, doi:10.1364/AO.38.004425, 1999.

Di Liberto, L., Cairo, F., Fierli, F., Di Donfrancesco, G., Viterbini, M., Deshler, T., and Snels, M.: Observation of polar stratospheric clouds over McMurdo (77.85^{o}S, 166.67^{o}E) (2006-2010), Journal of Geophysical Research: Atmospheres, 119, 5528–5541, doi:10.1002/2013JD019892, 2014.

Eyring, V., Shepherd, T. G., and Waugh, D. W.: SPARC CCMVal Report on the Evaluation of Chemistry-Climate Models, No. 5, 426 pp., 2010.

Garcia, R. R., Marsh, D. R., Kinnison, D. E., Boville, B. A., and Sassi, F.: Simulation of secular trends in the middle atmosphere, 1950-2003, Journal of Geophysical Research: Atmospheres, 112, n/a–n/a, doi:10.1029/2006JD007485, d09301, 2007.

Garcia, R. R., Smith, A. K., Kinnison, D. E., Cámara, l. d. l., and Murphy, D. J.: Modification of the Gravity Wave Parameterization in the Whole Atmosphere Community Climate Model: Motivation and Results, Journal of the Atmospheric Sciences, 74, 275–291, doi:10.1175/JAS-D-16-0104.1, https://doi.org/10.1175/JAS-D-16-0104.1, 2017.

Gobbi, G.: Lidar estimation of stratospheric aerosol properties - surface, volume, and extinction to backscatter ratio, Journal of Geophysical Research-Atmospheres, 100, 11 219–11 235, doi:10.1029/94JD03106, 1995.

Höpfner, M., Larsen, N., Spang, R., Luo, B. P., Ma, J., Svendsen, S. H., Eckermann, S. D., Knudsen, B., Massoli, P., Cairo, F., Stiller, G., v. Clarmann, T., and Fischer, H.: MIPAS detects Antarctic stratospheric belt of NAT PSCs caused by mountain waves, Atmospheric Chemistry and Physics, 6, 1221–1230, doi:10.5194/acp-6-1221-2006, 2006.

Hunt, W. H., Winker, D. M., Vaughan, M. A., Powell, K. A., Lucker, P. L., and Weimer, C.: CALIPSO Lidar Description and Performance Assessment, Journal of Atmospheric and Oceanic Technology, 26, 1214–1228, doi:10.1175/2009JTECHA1223.1, 2009.

Jourdain, L., Bekki, S., Lott, F., and Lefèvre, F.: The coupled chemistry-climate model LMDz-REPROBUS: description and evaluation of a transient simulation of the period 1980–1999, Annales Geophysicae, 26, 1391–1413, doi:10.5194/angeo-26-1391-2008, 2008.

Khosrawi, F., Kirner, O., Stiller, G., Höpfner, M., Santee, M. L., Kellmann, S., and Braesicke, P.: Comparison of ECHAM5/MESSy Atmospheric Chemistry (EMAC) simulations of the Arctic winter 2009/2010 and 2010/2011 with Envisat/MIPAS and Aura/MLS observations, Atmospheric Chemistry and Physics, 18, 8873–8892, doi:10.5194/acp-18-8873-2018, https://www.atmos-chem-phys.net/18/8873/2018/, 2018.

Kinnison, D. E., Brasseur, G. P., Walters, S., Garcia, R. R., Marsh, D. R., Sassi, F., Harvey, V. L., Randall, C. E., Emmons, L., Lamarque, J. F., Hess, P., Orlando, J. J., Tie, X. X., Randel, W., Pan, L. L., Gettelman, A., Granier, C., Diehl, T., Niemeier, U., and Simmons, A. J.: Sensitivity of chemical tracers to meteorological parameters in the MOZART-3 chemical transport model, Journal of Geophysical Research: Atmospheres, 112, n/a–n/a, doi:10.1029/2006JD007879, d20302, 2007.

Kirner, O., Ruhnke, R., Buchholz-Dietsch, J., Jöckel, P., Brühl, C., and Steil, B.: Simulation of polar stratospheric clouds in the chemistry-climate-model EMAC via the submodel PSC, Geoscientific Model Development, 4, 169–182, doi:10.5194/gmd-4-169-2011, https://www.geosci-model-dev.net/4/169/2011/, 2011.

Lamarque, J.-F., Kinnison, D. E., Hess, P. G., and Vitt, F. M.: Simulated lower stratospheric trends between 1970 and 2005: Identifying the role of climate and composition changes, Journal of Geophysical Research: Atmospheres, 113, n/a–n/a, doi:10.1029/2007JD009277, d12301, 2008.

Morgenstern, O., Giorgetta, M. A., Shibata, K., Eyring, V., Waugh, D. W., Shepherd, T. G., Akiyoshi, H., Austin, J., Baumgärtner, A. J. G., Bekki, S., Bräsicke, P., Brühl, C., Chipperfield, M. P., Cugnet, D., Dameris, M., Dhomse, S., Frith, S. M., Garny, H., Gettelman, A., Hardiman, S. C., Hegglin, M. I., Jöckel, P., Kinnison, D. E., Lamarque, J.-F., Mancini, E., Manzini, E., Marchand, M., Michou, M., Nakamura, T., Nielsen, J. E., Olivie, D., Pitari, G., Plummer, D. A., Rozanov, E., Scinocca, J. F., Smale, D., Teyssédre, H., Toohey, M., Tian, W., and Yamashita, Y.: Review of the formulation of present-generation stratospheric chemistry-climate models and associated external forcings, Journal of Geophysical Research: Atmospheres, 115, n/a–n/a, doi:10.1029/2009JD013728, d00M02, 2010.

Morgenstern, O., Hegglin, M. I., Rozanov, E., O'Connor, F. M., Abraham, N. L., Akiyoshi, H., Archibald, A. T., Bekki, S., Butchart, N., Chipperfield, M. P., Deushi, M., Dhomse, S. S., Garcia, R. R., Hardiman, S. C., Horowitz, L. W., Jöckel, P., Josse, B., Kinnison, D., Lin, M., Mancini, E., Manyin, M. E., Marchand, M., Marécal, V., Michou, M., Oman, L. D., Pitari, G., Plummer, D. A., Revell, L. E., Saint-Martin, D., Schofield, R., Stenke, A., Stone, K., Sudo, K., Tanaka, T. Y., Tilmes, S., Yamashita, Y., Yoshida, K., and Zeng, G.: Review of the global models used within phase 1 of the Chemistry–Climate Model Initiative (CCMI), Geoscientific Model Development, 10, 639–671, doi:10.5194/gmd-10-639-2017, 2017.

Noel, V., Hertzog, A., and Chepfer, H.: CALIPSO observations of wave-induced PSCs with near-unity optical depth over Antarctica in 2006-2007, Journal of Geophysical Research: Atmospheres, 114, n/a–n/a, doi:10.1029/2008JD010604, d05202, 2009.

Peter, T.: Microphysics and heterogeneous chemistry of polar stratospheric clouds, Annual Review of Physical Chemistry, 48, 785–822, doi:10.1146/annurev.physchem.48.1.785, pMID: 15012456, 1997.

Pitts, M. C., Poole, L. R., Lambert, A., and Thomason, L. W.: An assessment of CALIOP polar stratospheric cloud composition classification, Atmospheric Chemistry and Physics, 13, 2975–2988, doi:10.5194/acp-13-2975-2013, 2013.

Pitts, M. C., Poole, L. R., and Gonzalez, R.: Polar stratospheric cloud climatology based on CALIPSO spaceborne lidar measurements from 2006–2017, Atmospheric Chemistry and Physics Discussions, 2018, 1–54, doi:10.5194/acp-2018-234, 2018.

Pitts, M. C., Poole, L. R., and Thomason, L. W.: CALIPSO polar stratospheric cloud observations: second-generation detection algorithm and composition discrimination, Atmospheric Chemistry and Physics, 9, 7577–7589, 2009.

Pitts, M. C., Poole, L. R., Dörnbrack, A., and Thomason, L. W.: The 2009-2010 Arctic polar stratospheric cloud season: a CALIPSO perspective, Atmospheric Chemistry and Physics, 11, 2161–2177, doi:10.5194/acp-11-2161-2011, 2011.

Snels, M., Colao, F., Cairo, F., Scoccione, A., Muro, M. D., and Pitts, M.: Polar Stratospheric Cloud observations from Dome C (Antarctica) from 2014 to 2017, Atmospheric Chemistry & Physics, to be submitted, 2018.

Snels, M., Cairo, F., Colao, F., and Di Donfrancesco, G.: Calibration method for depolarization lidar measurements, International Journal of Remote Sensing, 30, 5725–5736, doi:10.1080/01431160902729572, 2009.

Solomon, S., Kinnison, D., Bandoro, J., and Garcia, R.: Simulation of polar ozone depletion: An update, Journal of Geophysical Research: Atmospheres, 120, 7958–7974, doi:10.1002/2015JD023365, 2015.

Stephens, G., Winker, D., Pelon, J., Trepte, C., Vane, D., Yuhas, C., L'Ecuyer, T., and Lebsock, M.: CloudSat and CALIPSO within the A-Train: Ten years of actively observing the Earth system, Bulletin of the American Meteorological Society, 0, null, doi:10.1175/BAMS-D-16-0324.1, 2017.

Stephens, G. L., Vane, D. G., Boain, R. J., Mace, G. G., Sassen, K., Wang, Z., Illingworth, A. J., O'Connor, E. J., Rossow, W. B., Durden, S. L., Miller, S. D., Austin, R. T., Benedetti, A., Mitrescu, C., and Team, T. C. S.: THE CLOUDSAT MISSION AND THE A-TRAIN, Bulletin of the American Meteorological Society, 83, 1771–1790, doi:10.1175/BAMS-83-12-1771, 2002.

Wang, Z., Stephens, G., Deshler, T., Trepte, C., Parish, T., Vane, D., Winker, D., Liu, D., and Adhikari, L.: Association of Antarctic polar stratospheric cloud formation on tropospheric cloud systems, Geophysical Research Letters, 35, n/a–n/a, doi:10.1029/2008GL034209, l13806, 2008.

Wegner, T., Kinnison, D. E., Garcia, R. R., and Solomon, S.: Simulation of polar stratospheric clouds in the specified dynamics version of the whole atmosphere community climate model, Journal of Geophysical Research: Atmospheres, 118, 4991–5002, doi:10.1002/jgrd.50415, http://dx.doi.org/10.1002/jgrd.50415, 2013.

Winker, D. M., Vaughan, M. A., Omar, A., Hu, Y., Powell, K. A., Liu, Z., Hunt, W. H., and Young, S. A.: Overview of the CALIPSO Mission and CALIOP Data Processing Algorithms, Journal of Atmospheric and Oceanic Technology, 26, 2310–2323, doi:10.1175/2009JTECHA1281.1, 2009.

Zhu, Y., Toon, O. B., Lambert, A., Kinnison, D. E., Brakebusch, M., Bardeen, C. G., Mills, M. J., and English, J. M.: Development of a Polar Stratospheric Cloud Model within the Community Earth System Model using constraints on Type I PSCs from the 2010–2011 Arctic winter, Journal of Advances in Modeling Earth Systems, 7, 551–585, doi:10.1002/2015MS000427, http:https://doi.org/10.1002/2015MS000427, 2015.

Zhu, Y., Toon, O. B., Lambert, A., Kinnison, D. E., Bardeen, C., and Pitts, M. C.: Development of a Polar Stratospheric Cloud Model Within the Community Earth System Model: Assessment of 2010 Antarctic Winter, Journal of Geophysical Research: Atmospheres, 122, 10,418–10,438, doi:10.1002/2017JD027003, 2017JD027003, 2017a.

Zhu, Y., Toon, O. B., Pitts, M. C., Lambert, A., Bardeen, C., and Kinnison, D. E.: Comparing simulated PSC optical properties with CALIPSO observations during the 2010 Antarctic winter, Journal of Geophysical Research: Atmospheres, 122, 1175–1202, doi:10.1002/2016JD025191, 2016JD025191, 2017b.